

## BANDGAP OPTIMIZATION OF ABSORBER LAYERS IN AMORPHOUS SILICON SINGLE AND MULTIJUNCTION JUNCTION SOLAR CELLS

M. I. KABIR<sup>a</sup>, ZAHARI IBARAHIM<sup>b</sup>, M. ALGHOUL<sup>b</sup>, KAMARUZZAMAN SOPIAN<sup>b</sup>, MD. REZAUL KARIM<sup>c</sup>, NOWSHAD AMIN<sup>a,b,c\*</sup>

<sup>a</sup>*Department of Electrical, Electronics and Systems Engineering, Faculty of Engineering and Built Environment*

<sup>b</sup>*Solar Energy Research Institute (SERI), Universiti Kebangsaan Malaysia, Bangi, Selangor, Malaysia*

<sup>c</sup>*Center of Excellence for Research in Engineering Materials (CEREM), College of Engineering,*

*King Saud University, Riyadh 11421, Saudi Arabia*

Single and multijunction amorphous silicon thin film solar cells have been investigated here by the Analysis of Microelectronic and Photonic Structures (AMPS 1D) simulator in regard to overall performance. The photovoltaic characteristics have been observed by changing the bandgap of the absorber layers, variation of light intensity and the effect of operating temperature for single and multijunction devices. The absorber layer a-SiO:H in single junction cell has shown better efficiency trend within the bandgap range of 1.8-2.2 eV and the highest efficiency of 17.67% is achieved at 2 eV. Moreover, efficiency of 17.95% has been found at 10 suns. The second absorber layer a-SiC:H in double junction cell shows the highest efficiency of 19.04% at 1.9 eV. In contrast, the maximum efficiency of 20.42% has been found for the bandgap of 1.8 eV in a-Si:H as absorber layer of the bottom cell in triple junction configuration. For double and triple junctions, the efficiency increased to 21.94% and 25.58% at 30 and 100 suns, respectively. The temperature gradients for single, double and triple junction are found to be -0.17%/°C, -0.20%/°C and -0.28%/°C, respectively.

(Received November 18, 2011; Accepted January 16, 2012)

*Keywords:* Single junction; multijunction; absorber layer; bandgap; operating temperature, Light intensity and AMPS-1D

### 1. Introduction

The hydrogenated amorphous silicon (a-Si:H) pin solar cell has been extensively investigated since its invention by Carlson and Wronski [1]. These extensive investigations are mainly due its continuous advancement in photovoltaic research and development. Amorphous silicon (a-Si) alloys have now become an attractive avenue in thin film technology mainly due to its material availability, ease of fabrication as well as for large scale production capability [2]. The disordered nature of the a-Si material gives it greater flexibility in tailoring improved photovoltaic properties and solar cell structures [3]. The large area deposition at relatively low temperatures on a variety of substrates facilitates the mass production. The conversion efficiency of hydrogenated amorphous silicon (a-Si:H) thin film solar cells has gradually been improved from 2.4% to 15.2% [1,4-8]. These improvements have been possible by applying different device design techniques, new materials having higher optoelectronic properties and manufacturing processes sustained progress in a-Si:H based technologies. However, light induced effect on a-Si was first reported by

---

\*Corresponding author:nowshad@eng.ukm.my

Staebler and Wronski from the beginning of a-Si based solar cells research. Obviously, it has significantly improved and still it is an impediment for higher stabilized efficiencies [5, 9-10].

For improvement in stabilized a-Si solar cells efficiency needs adapted cell designs and advanced light trapping concepts [11]. In order to avoid light induced degradation, multijunction device approach has been initiated with the targets of higher efficiencies not only in initial state but also for stabilized state [4, 7]. The multijunction device uses thin intrinsic layers with different optical bandgaps which leads to absorption of a larger part of the solar spectrum. Each sub-cell has to be optimized separately with different parameters. The spectrum of the solar photons reaching the earth's surface covers a wide range of wavelength from 0.3 to 2.0  $\mu\text{m}$  (corresponding to 0.6-4 eV in energy). However, a-Si:H has an optical gap of about 1.7 eV, and will not absorb photons below that energy. In order to increase the photon absorption profoundly in multijunction solar cell the absorber layer from top to bottom cell should gradually be narrowed.

Bandgap of a-Si alloys can be varied in a wide range (1.1 to 3.7 eV) by the incorporation of hydrogen, oxygen, carbon, and germanium etc. The bandgaps of a-SiC:H and a-SiO:H alloys can be tuned from 1.7 to more than 4.2 eV by changing the carbon and oxygen contents which can be used in absorber layers of the top cell in tandem structures [12,13].

In this study, we have designed three types of solar cell models with single, double and triple junctions having the structure of 1)  $\mu\text{c-SiO:H/a-SiO:H/a-Si:H}$ ; 2)  $\mu\text{c-SiO:H/a-SiO:H/a-Si:H}/\mu\text{c-SiO:H/a-SiC:H/a-Si:H}$  and 3)  $\mu\text{c-SiO:H/a-SiO:H/a-Si:H}/\mu\text{c-SiO:H/a-SiC:H/a-Si:H/a-Si:H}$ , respectively. In practice, the single junction cell usually does not give higher efficiency due to the leakage of maximum energy utilization of sunlight. Consequently, we have designed the multijunction solar cells such as double and triple junctions based on the spectral splitting principle so that the maximum energy can be absorbed. Moreover, the light induced degradation i.e., higher instability in single junction leads us to design stacked structure for capturing the solar spectrum efficiently, then it can achieve the maximum conversion efficiency [14]. The solar concentration can be another technique to improve the performance of solar cells which we have investigated with the variation of light intensity [15].

## 2. Experimental: simulation of the devices

Simulation technique offers a conventional tool not only for an optimum device design but also for performance analysis of the physical device. AMPS-1D is a very general computer simulation code developed by a group from Pennsylvania State University for analyzing and designing two terminal structures [16]. The one-dimensional device simulation program AMPS-1D solves the Poisson's equation and the electron and hole continuity equations by using finite differences and the Newton-Raphson technique. The AMPS-1D analyzes the transport behaviors of the semiconductor and opto-electric devices, along with an appropriate boundary condition. It can handle devices such as p-n and p-i-n homo- and hetero-junctions, p-i-p and n-i-n structures etc.

The single and multijunction p-i-n structure solar cell models have been designed and analyzed the performance in respect to the  $V_{oc}$ ,  $J_{sc}$  and FF and efficiency by incorporating the material parameters into AMPS-1D which is shown in Figure 1. The values of different material parameters fed into AMPS-1D are shown in Table 1 and Table 2.

In the device modelling, we used wide bandgap  $\mu\text{c-SiO:H}$  in top and middle cell and a-SiC:H in bottom cell as a window layers (p-layer) for the absorption of maximum incident photon energy. The wider bandgap materials facilitate to increase the  $V_{oc}$  and  $J_{sc}$  of the devices. It is well known that  $V_{oc}$  is sensitive to p-layer and p/i interface as evident in hetero-junction solar cell. Since optical absorption at the p-layer limits  $J_{sc}$ , wider optical gap material is always desired for this purpose [17].

The absorber layers that has been chosen for single, double and triple junctions are a-SiO:H, a-SiC:H and a-Si:H, respectively. Amorphous SiO:H is more stable in high temperature environment and is better for gaining high  $V_{oc}$  in triple junction cell as top absorber layer [18]. The medium energetic photons will be absorbed in a-SiC:H and low energetic photons will be absorbed in bottom absorber layer of a-Si:H. The maximum energy will be received in top and middle cells and their light induce degradation is less than a-Si:H. So the effect of light induced

degradation contributes in triple junction configuration mostly from the bottom cell. The a-Si:H has been chosen as n-layer for single, double and triple junction. In p-i-n junction solar cell p and n-layer build an electric field across the absorber i-layer. The incident light which passes through p-layer and absorbed in i-layer creates electrons and holes, which are separated by the electric field. So the role of i-layer for p-i-n junction is very important.

The front and back contact of the model have been inserted accordingly. In this device, we used indium tin oxide (ITO) as a front contact and all of their optical parameters (as shown in Table 2) were used in the simulation. The indium tin oxide (ITO) is not only highly transparent and good electrical conductor but it also provides the most compatible physical and electronic interface properties. The resistivity of ITO is as low as  $2.3 \times 10^{-4} \Omega\text{-cm}$  and optical transmittance in the visible wavelength range above 90% [19]. Moreover, a key advantage of ITO is that it is physically stable and chemically inert, so it does not make any chemical reaction with its surrounding layer.

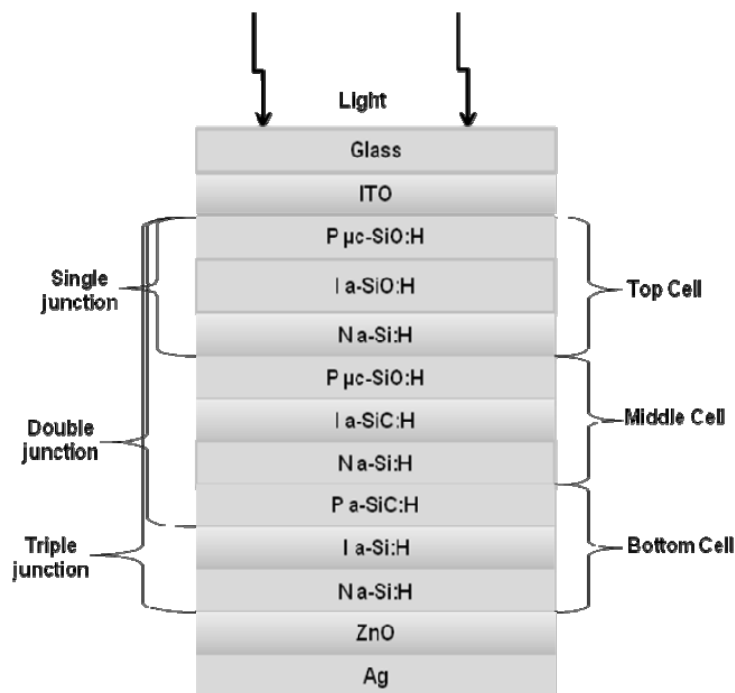


Fig. 1. Structural view of a-Si based solar cells (generalized).

Silver is inserted as back contact for its low resistivity ( $2 \times 10^{-6} \Omega\text{-cm}$ ) to reduce the reflection losses through all layers. To increase the  $J_{sc}$ , the low resistive ( $2.6 \times 10^{-2} \Omega\text{-cm}$ ) and high optical transparent ZnO layer is applied between n-layer and Ag as transparent back contact [20]. However, ZnO/Ag has the capability to overcome the adhesion problem between a-Si and metal contact [21]. After setting all the parameters, simulation was carried out and the results were obtained and compared.

Table 1. Overall electronic properties used in simulation

Material/parameters	P ( $\mu\text{c-SiO:H/a-SiC:H}$ )	I ( $\text{a-SiO:H/a-SiC:H/a-Si:H}$ )	N ( $\text{a-Si:H}$ )
Relative permittivity, $\epsilon_r$	11.9	11.9	11.9
Electron mobility, $\mu_n$ ( $\text{cm}^2/\text{Vs}$ )	10.0	20.0	20.0
Hole mobility, $\mu_p$ ( $\text{cm}^2/\text{Vs}$ )	1.0	2.0	2.0
Acceptor & donor concentration ( $\text{cm}^{-3}$ )	$N_A=$ $3.0 \times 10^{18}$	-	$N_D=$ $8.0 \times 10^{18}$
Bandgap (eV)	1.8-2.3	1.8-2.3	1.65-1.85
Effective density of states in conduction band ( $\text{cm}^{-3}$ )	$2.5 \times 10^{20}$	$2.5 \times 10^{20}$	$2.5 \times 10^{20}$
Effective density of states in valance band ( $\text{cm}^{-3}$ )	$2.5 \times 10^{20}$	$2.5 \times 10^{20}$	$2.5 \times 10^{20}$
Electron affinity (eV)	3.8	3.8	3.8

Table 2. General layer parameters

Parameters	Front Contact	Back Contact
Barrier height, ( $\phi_{bo}/\phi_{bl}$ )	PHIBO=1.9 eV	PHIBL=0.3 eV
Electron recombination speed	SNO= $1 \times 10^7$ cm/s	SLN= $1 \times 10^7$ cm/s
Hole recombination speed	SPO= $1 \times 10^7$ cm/s	SPL= $1 \times 10^7$ cm/s
Reflection coefficient	RF=0.1	RB=0.9

### 3. Results and discussion

#### 3.1 Effect of Bandgap in Cell Performance

To find the optimum structure of a-Si solar cells in single and multijunction approach, the bandgap of absorber layers has been varied in the range of 1.8 to 2.3 eV. Bandgap of each layer has to decrease from top to bottom cell to absorb various types of energetic photons. Figure 2 represents the single, double and triple junction solar cell performance with the change of bandgap of a-SiO:H, a-SiC:H and a-Si:H in the range of 1.8 eV to 2.3 eV. The  $V_{oc}$ ,  $J_{sc}$  and FF are in good trend in double and triple junction configurations hence the efficiency of these cells change almost in the same way. For single junction, the change of  $V_{oc}$  and  $J_{sc}$  are almost in same trend but FF gradually decreases after 2.1 eV. Hence the efficiency decreases sharply after the bandgap value of 2.1 eV due to the decrease of photoconductivity and photosensitivity. As the bandgap increases more than 2 eV in double junction configuration, the cell efficiency decreases gradually due to the decrease of the  $V_{oc}$ ,  $J_{sc}$  and FF. It could be attributed to the increase of defect density due to the increase of carbon incorporation for increasing bandgap and eventually photoconductivity decreases. It has been found that the efficiency trend for triple junction is quite good in the bandgap range of 1.8 eV to 1.9 eV for the absorber layer of bottom cell. Afterwards the efficiency falls sharply due to the decrease of  $J_{sc}$  and FF. Obviously, in triple junction configuration the bottom cell gets the chance to convert the low energetic photons into electron-hole pairs that are passing through the top cells. Fig. 3 shows the electric field distribution profile for single, double and triple junction a-Si solar cells.

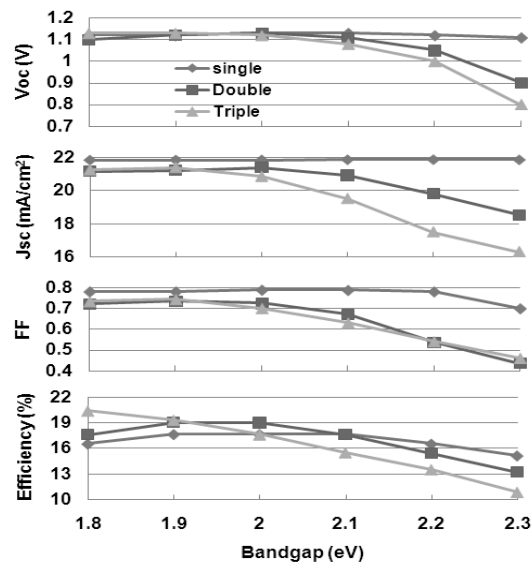


Fig 2. Effect of bandgap in cell performance

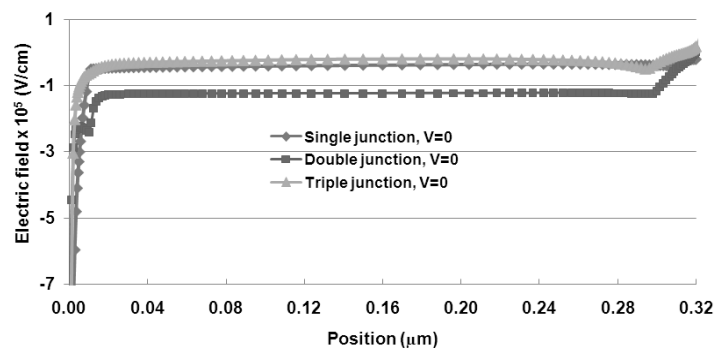


Fig. 3. Electric field distribution of *a*-Si solar cells with *p-i-n* configuration

### 3.2 Current Density and Quantum Efficiency

Figure 4 has shown the J-V characteristics curve for single, double and triple junction amorphous silicon solar cells. The highest  $J_{sc}$  for single, double and triple junction solar cells are  $20.86 \text{ mA/cm}^2$ ,  $20.47 \text{ mA/cm}^2$ , and  $20.23 \text{ mA/cm}^2$ , respectively. This fact also ensures the current matching in all cells of the multi-junction configurations. The highest  $V_{oc}$  for single, double and triple junction solar cells are 1.05V, 1.13V and 1.21V, respectively.

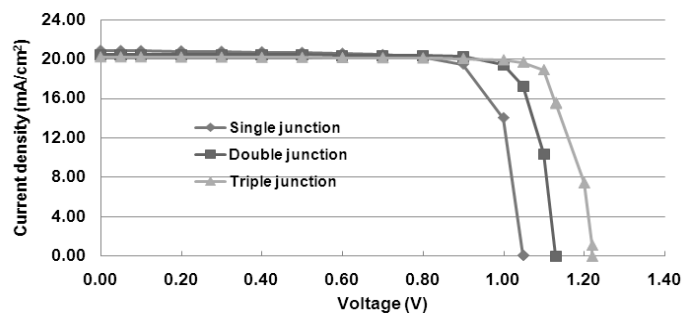


Fig. 4. J-V characteristics of *a*-Si solar cells with various configurations

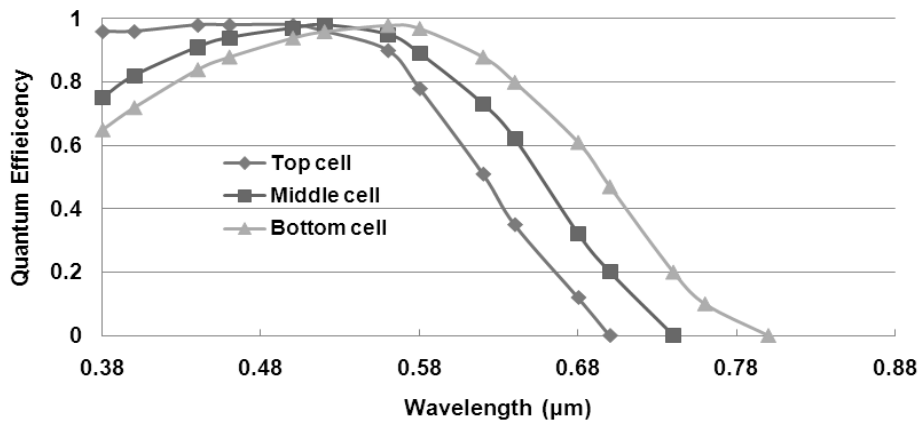


Fig. 5. Spectral response of a-Si solar cells.

Figure 5 shows the spectral response for p-i-n configured single and multijunction solar cells. The high, medium and low energetic photons have been absorbed in top, middle and bottom cells, respectively. It has been observed that the quantum efficiency is increased up to an average of 20% in red zone of the spectrum with the increase of cell levels, it occurs due to the decrease of band gap of different layers from top to bottom cells while increased the absorption of light spectrum. However, the triple junction cell here has absorbed approximately total spectrum in visible range, hence the cell efficiency has increased.

### 3.3 Effect of Light Intensity on Cell Performance

Figure 6 illustrates the performance of single, double and triple junction a-Si solar cells in respect to the exposed light intensity ranging from 0.01 to 100 suns. For single junction, the FF and  $J_{sc}$  per intensity show the decreasing trend with the increase of light intensity; whereas  $V_{oc}$  shows the increasing nature with intensity. The highest efficiency of 17.95% has been found at 10 suns. Overall performance of the single junction a-Si solar cell has been improved compared with 1 sun exposure in light. The general trend is an increase in cell efficiency with increasing concentration ratio for lower light exposure and decrease in cell efficiency at higher intensity. The maximum efficiency has been found at around 5 to 15 suns. At high current density, series resistance loss becomes prominent and affects the efficiency by decreasing the FF.

In the case of double junction, the FF and  $V_{oc}$  are in the continuous increasing trend with the increase of light intensity whereas  $J_{sc}$  per intensity reaches its highest value at 1 sun. However, after 10 suns it shows a saturated value. In case of double junction configuration the cell efficiency has significantly been improved with the increase of light exposure and it reaches the highest value of 21.94% at 30 suns.

In triple junction solar cell, the  $V_{oc}$  increases with the increase of light intensity whereas  $J_{sc}$  per intensity reaches in saturation at 10 suns. The efficiency shows a continuous increasing trend from 10 suns to 100 suns. The maximum efficiency of 25.58% has been achieved at 100 suns. These higher efficiencies will eventually lead to the high production costs as solar concentrating systems are still complex and costly. This allows relatively complex schemes for increasing photovoltaic efficiency to be implemented.

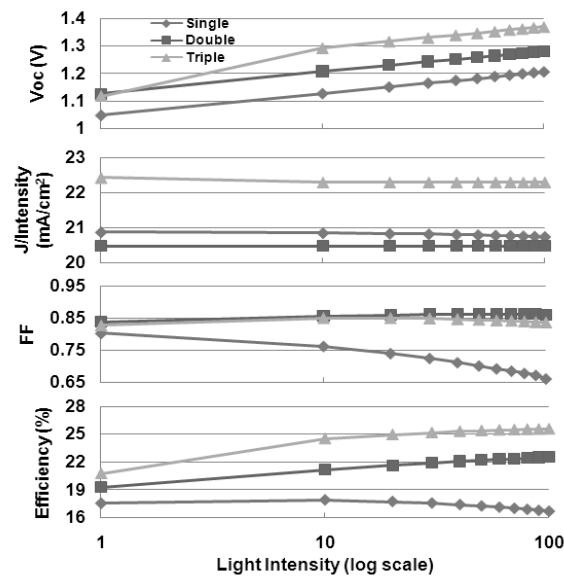


Fig. 6. Effect of light intensity on cell performance.

### 3.4 Effect of Temperature on Bandgap

The energy bandgap of semiconductors tends to decrease with increasing temperature. When temperature increases, the amplitude of atomic vibrations increase, leading to larger interatomic spacing and also increase the interaction of the free electrons and free holes as well as recombination of electron-hole pairs [22]. In reality, it is well known that the efficiency of Si based solar cell decrease with the increase of light exposure time due to increase of operating temperature of the cells. The increase of temperature changes the physical properties of the cell layers as shown in Figure 7. It has been observed that the valance and conduction bands shift with the increase of temperature. The interaction between the lattice and the free electrons and holes will also affect the band gap to a smaller extent [23].

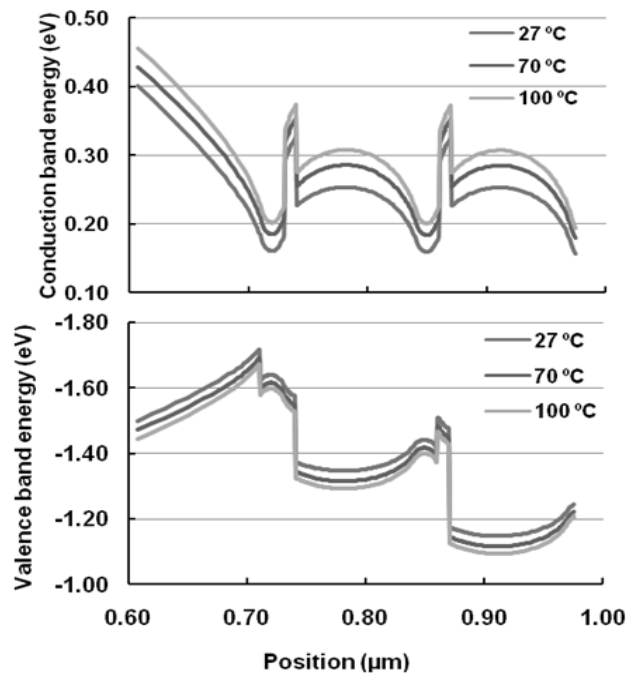


Fig. 7. Band splitting due to temperature effect for triple junction in conduction and valence bands

### 3.5 Effect of Operating Temperature on Cell Performance

The effect of temperature on amorphous silicon based solar cell is the major concerning fact regarding the improvement of efficiency as well as better stabilities. The overall performance of single, double and triple junction a-Si based solar cell has been shown in Figure 8. The temperature gradients for single, double and triple junction are  $-0.17\%/^{\circ}\text{C}$ ,  $-0.20\%/^{\circ}\text{C}$  and  $-0.28\%/^{\circ}\text{C}$ , respectively. These result indicates that a-SiO:H is more stable comparing with a-SiC:H and a-Si:H. The temperature gradient for triple junction reveals that a-Si:H will impose higher instability in efficiency than wider bandgap a-SiO:H and a-SiC:H. However, microcrystalline silicon ( $\mu\text{c-Si}$ ) does not show the photo degradation that is an advantage over amorphous silicon. But  $\mu\text{c-Si}$  has a drawback of lower  $V_{oc}$  which limits the efficiency compared to the single or multi-crystalline silicon solar cells. [24].

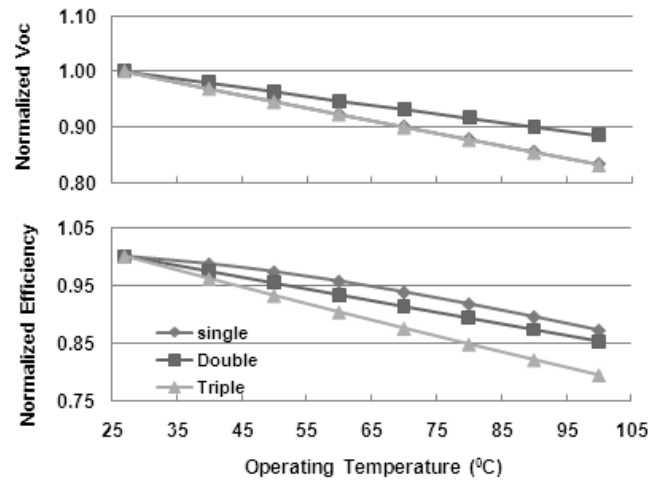


Fig. 8. Effect of operating temperature on cell performance

## 4. Conclusion

The maximum efficiency of 17.67% has been achieved with an absorber layer bandgap of 2 eV for single junction solar cells. For double junction, the highest efficiency of 19.04% has been found for middle cell's absorber layer bandgap of 1.9 eV and triple junction cell shows the highest efficiency of 20.42% with the bottom cell's absorber layer bandgap of 1.8 eV. The simulation results show that the optimum bandgap for a-SiO:H, a-SiC:H and a-Si:H as window layers in single, double and triple junction configuration are 2 eV, 1.9 eV and 1.8 eV, respectively. The maximum efficiency for single junction (17.95%) observed at 10 suns whereas efficiency of the double and triple junctions are 21.94% and 25.58% at 30 and 100 suns. Though the solar concentrating technique has significantly improved the efficiencies of these devices in simulation, practical investigation is needed for verification. If the simulated and experimental results match well then it will be a significant achievement in context to reduce material cost. These three models can be tried for fabrication in laboratory in order to achieve higher performance at cost-effective fabrication processes. It is evident from this numerical simulation that the triple junction structure with the proposed configuration shows the best performance in comparison with the single and double junction configurations.

## Acknowledgment

This work is supported by the Solar Energy Research Institute (SERI) of the National University of Malaysia (UKM) through the research grant UKM-GUP-BTT-07-29-184.

## References

- [1] D. E. Carlson and C. R. Wronski, Amorphous silicon solar cell, *Appl. Phys. Lett.*; **28**(11), 671 (1976)
- [2] S. K. Deb, Recent developments in high-efficiency PV cells, World Renewable Energy Congress (WREC) VI, Brighton, U.K. July 1-7, 2000, pp 1-9.
- [3] D.Y.N. Kim, I. S. Kim, S. Y. Choi, *Solar Energy Mater & Solar Cells*; **93**: 239 (2009).
- [4] J. Yang, A. Banerjee, S. Guha, *Appl. Phys. Lett.*; **70** (22): 2975 (1997).
- [5] J. Meier, S. Dubail, J. Cuperus, U. Kroll, R. Platz, P. Torres, J.A. Anna Selvan, P. Pernet, N. Beck, N. Pellaton Vaucher, Ch. Hof, D. Fischer, H. Keppner, A. Shah, *J. Non-Cryst. Solids*; **227–230**, 1250 (1998).
- [6] S. Tsuda, T. Takahama, Y. Hishikawa, H. Tarui, H. Nishiwaki, K. Wakisaka S. Nakano, *J Non-Cryst Solids*; **164-166**(2), 679 (1993).
- [7] S. Guha, The triple junction a-Si:H/a-SiGe:H/a-SiGe:H solar cell shows an efficiency of 13.7%. *Appl Phys Lett*; **54**, 2333 (1984).
- [8] A. Kolodziej, C. R. Wronski, P. Krewniak, S. Nowak, Silicon thin film multijunction solar cells. *Opto-electronics Review*; **8**(4), 339 (2000).
- [9] D.L. Staebler, C. R. Wronski, *Appl Phys Lett*; **31**, 292 (1977).
- [10] T. Wada, M. Kondo and A. Matsuda, *Solar Energy Mater Solar Cells*; **74**, 533-538 (2002).
- [11] Shah AV, Vaněček M, Meier J, Meillaud F, Guillet J, Fischer D, Droz C, Niquille X, Faÿ S, Sauvain EV, Daudrix VT, Bailat J. Basic efficiency limits, recent experimental results and novel light-trapping schemes in a-Si:H,  $\mu$ c-Si:H and ‘micromorph tandem’ solar cells. *J. Non-Cryst. Solids*; **338-340**, 639 (2004).
- [12] Y. Tawada, K. Tsuge, M. Kondo, H. Okamoto, Y. Hamakawa, *J. Appl. Phys.* **53**, 5273 (1982).
- [13] S.M. Iftiqar, The roles of deposition pressure and RF power in opto-electronic properties of a-SiO:H films, *J. Phys. D: Appl. Phys.*; **31**, 1630 (1998).
- [14] L. Lei, Y. K. Chae, S. Sheng, T. K. Won, A. Kadam, J. Chen, S.Y. Choi, and J. M. White, a-Si:H single junction and a-Si:H/C-Si:H tandem solar cells fabrication using large area (5.7m<sup>2</sup>) PECVD systems, Technical Digest of the International PVSEC-17. 2007, Fukuoka, Japan.
- [15] E. Kussul, T. Baidyk, O. Makeyev, F. Lara-Rosano, J. M. Saniger and N Bruce, Flat facet parabolic solar concentrator. 2<sup>nd</sup> WSEAS/IASME International Conference on Renewable Energy Sources (Res’08). Corfu, Greece, October 26-28, 2008.
- [16] S. V. FonAsh, J. Arch, J. Cuiffi, J. Hou, W. Howland, P. McElheny, A. Moquin, M. Rogosky, F. Rubinelli, T. Tran, and H. Zhu, A manual for AMPS-1D for windows 95/NT; a one-dimensional device simulation program for the analysis of microelectronic and photonic structures. 1997, Pennsylvania State University, USA.
- [17] T. Itoh, K. Fukunaga, Y. Katoh, T. Fujiwara, S. Nonomura, *Solar Energy Mater & Solar Cells*; **74**, 379 (2002).
- [18] B. G. Yacobi, R. W. Collins, G. Moddel, P. Viktorovitch, W. Paul, *Phys. Rev. B* **24**: 5907–(1981).
- [19] A. N. H. Al-Ajili and S. C. Bayliss, *Thin Solid Films*; **305**: 116-123 (1997).
- [20] H. Afifi, H. M. Abdel-Naby, S. El-Hefnawie, A. Eliewa, and N. Ahmad, *Wseas Transactions On Electronics*; **4**(2), 180 (2005).
- [21] K. Hayashi, M. Kondo, A. Ishikawa, and H. Yamagishi, ZnO/Ag sputtering deposition on a-Si solar cells, First WCPEC, Dec. 5-9, 1994, Hawaii, USA.
- [22] H. Unlu, *Solid State Electronics*; **35**, 1343 (1992).
- [23] K. P. O’Donnell, and X. Chen, Temperature dependence of semiconductor band gaps, *Appl. Phys. Lett.*; **58**: 25 (1991).
- [24] H. Takakura and Y. Hamakawa, *Solar Energy Mater & Solar Cells*. **74**, 479 (2002).